

Enhanced Proton Conductivity as Bio-Based Electrolyte Membranes in Fuel Cell Application: The Role of Sulfonated Graphitic Carbon Nitride

Yusra Nadzirah Yusoff¹, Norazuwana Shaari^{1,*}, Ajaz Ahmad Wani^{1,2}, Mohamad Azuwa Mohamed³, Kee Shyuan Loh¹, Siti Kartom Kamarudin^{1,4}, Roshasnorlyza Hazan⁵, Je-deok Kim⁶

¹ Fuel Cell Institute, Universiti Kebangsaan Malaysia, 43600 UKM Bangi, Selangor, Malaysia

² Department of Chemistry, Aligarh Muslim University, Aligarh, India

³ Department of Chemicals Science, Faculty of Science and Technology, Universiti Kebangsaan Malaysia, 43600 UKM Bangi, Selangor, Malaysia

⁴ Department of Chemical and Process Engineering, Faculty of Engineering and Built Environment, Universiti Kebangsaan Malaysia, 43600 UKM Bangi, Selangor, Malaysia

⁵ Materials Technology Group, Industrial Technology Division, Malaysian Nuclear Agency, Bangi, 43000 Kajang, Selangor, Malaysia

⁶ Environmental Circulation Composite Materials Group, Functional Materials Field, Research Center for Electronics and Optical Materials, National Institute for Materials Science, 1-1 Namiki, Tsukuba, 305-0044, Japan

ARTICLE INFO

Article history:

Received 1 November 2024

Received in revised form 6 December 2024

Accepted 8 January 2025

Available online 31 March 2025

Keywords:

Sodium alginate; sulfonated graphitic carbon nitride; biocomposite membrane; DMFC

ABSTRACT

Nafion is a commercial polymer membrane commonly used in direct methanol fuel cell (DMFC) systems, despite its major limitations such as high fuel crossover and high manufacture cost. The production of sodium alginate (SA) blended membrane with modification by graphitic carbon nitride (gCN) and sulfonated graphitic carbon nitride (S-gCN) as an inorganic filler is one of several current efforts to discover an alternative membrane. In this study, SA/S-gCN and SA/gCN biocomposite membranes were prepared using solution casting method and dried at certain temperature. The SA/S-gCN and SA/gCN biocomposite membranes outperform the pure SA membrane based on water uptake, swelling ratio, ion exchange capacity, and proton conductivity results. The distinct features of SA and S-gCN filler create good intercalation, thus producing new materials with excellent performance. The maximum proton conductivity reported in this study is $8.67 \times 10^{-3} \text{ S cm}^{-1}$, which was obtained at room temperature using SA/S-gCN membrane. The interaction of biomembrane composite was investigated via water uptake and swelling ratio studies. Results showed that the designed SA/S-gCN and SA/gCN have a low water uptake and swelling ratio compared to that of pure SA membrane (84% water uptake and 72% swelling ratio). As a result, the membrane developed in this study shows significant potential as an alternative membrane for future usage in DMFC applications.

1. Introduction

Fossil fuels have consistently been in high demand for energy supply in recent years, as they are both readily available and inexpensive. They are exclusively employed to generate electricity.

* Corresponding author.

E-mail address: norazuwanashaari@ukm.edu.my

<https://doi.org/10.37934/kijbb.1.1.113>

Nevertheless, the world is currently experiencing a scarcity of fossil fuels, so it is imperative to identify alternative energy sources. Sustainability, or "green" energy, has gained popularity in addition to the environmental consequences of global warming and other climate changes. One of the prospective energy sources that is considered carbon neutral is renewable energy, such as biomass. As an additional consequence of these circumstances, fuel cells that historically have utilized high-value metal catalysts to produce electricity have garnered significant attention as alternative energy sources [1]. Fuel cells notably surpass other energy generation methods due to their lack of emissions, including sulphur dioxide and carbon dioxide, as well as their superior efficiency. Fuel cell technology is an efficient technology that meets global energy needs without having adverse effects on the environment. Hydrogen, methane, methanol, ethanol, formic acid, sodium borohydride, biomass, coal, and glucose are among the examples of fuel sources commonly used in producing electricity [2,3]. Among these sources, liquid fuels such as methanol and ethanol have benefits in terms of cost-effectiveness, minimal manufacturing expenses, and high energy efficiency. Direct Methanol Fuel Cell (DMFC) is considered as one clean energy technology since it can produce electricity via chemical reactions, without traditional combustion methods. DMFCs are used in many applications such as mobile devices, medical devices, hearing aids, home appliances, cars, and more [4]. The significance of commercializing this technology has escalated because of the current surge in worldwide demand. Nevertheless, the DMFC system encounters certain constraints that impede its commercialization, including suboptimal efficiency (reaching a maximum of around 60%) and substantial manufacturing expenses, mostly due to the use of the costly commercial Nafion membrane [5].

The polymer electrolyte membrane (PEM) is a crucial component in the DMFC system. This has led researchers to pursue significant improvements in the quest for alternative membranes that are more economically efficient and possess equivalent capabilities to the Nafion membrane [6]. Biopolymers such as alginate, carrageenan, chitosan, and cellulose have found extensive usage in many applications. However, their suitability for DMFC applications, particularly as PEM, is rather restricted. Biopolymers have the benefit of cost-effectiveness as a result of their abundant availability, capacity to decompose naturally, ease of being molded into diverse shapes, and environmental friendliness. Sodium alginate (SA) is a type of biopolymer readily obtained from the ocean, comprising various species, including brown and green algae species depending on their breeding habitat [7]. SA, obtained from marine algae, is a non-toxic anionic biopolymer consisting of β -D-mannuronate (M) and α -L-guluronate (G) in diverse proportions [8]. SA is also a polysaccharide that serves as a membrane material with selective water absorption in the application of pervaporation of azeotropic mixtures. Nonetheless, the pristine SA membrane exhibits excessive swelling and inadequate mechanical stability, limiting its application in PEMs for DMFCs. Previously, SA has been widely used as a food coating and in medical devices due to its natural properties [9]. Some previous studies have employed SA polymer as an electrolyte membrane and achieved higher power values than other biomembranes. SA polymer was also found to have significant potential for developing an electrolyte membrane in fuel cell technology. However, its limitations in terms of high water absorption, poor proton conductivity, and low mechanical strength necessitate further modification to make it suitable for DMFC applications.

To address these limitations, additives such as fillers, cross-linking agents, and plasticizing agents are widely used to enhance the characteristics of SA polymer [10,11]. However, the integration of advanced materials like sulfonated graphitic carbon nitride (S-gCN) with SA membranes remains unexplored. For example, Ping-Ping et al., used graphene oxide (GO) as an additive to enhance the mechanical characteristics of carrageenan membranes [12]. Zhang *et al.*, proved the effectiveness of glutaraldehyde as a cross-linking agent in improving the mechanical characteristics of chitosan

membranes [13]. Furthermore, the presence of plasticizing agents could also enhance the flexibility and proton conductivity of polymer membranes [14].

Graphitic carbon nitride (g-CN) is a stable two-dimensional layered material that has similarities with graphene. It is composed of tri-s-triazine units that are interconnected by amino groups. Presently, g-CN is extensively used in diverse applications, particularly in photocatalysis for the degradation of pollutants and the reduction of CO₂. These properties may be ascribed to its stable electrical structure, as well as its strong thermal and chemical resistance [15]. In addition, g-CN has been investigated for its ability to change the SPEEK polymer, resulting in improved proton conductivity and decreased methanol crossover [16]. When g-CN is in its bulk state, it has several disadvantages, such as the tendency to form non-uniform aggregates that may agglomerate owing to strong van der Waals interactions (specifically, π - π stacking). To address this issue, various surface modifications of g-CN have been attempted to enhance its dispersibility. Sulfonated gCN (S-gCN) have also been utilized to modify polymer membranes, aiming to improve membrane performance. The potential of S-gCN as a filler for biopolymers like SA to fabricate PEMs for DMFC applications has not been reported. To the best of our knowledge, no study has explored the fabrication and comprehensive evaluation of SA/S-gCN membranes for DMFCs, including crucial parameters such as water absorption, swelling ratio, proton conductivity, and ion exchange capacity. This leaves a significant void in understanding the practical viability of these composites for fuel cell applications.

Therefore, this work aims to investigate the significant potential of incorporating S-gCN as in inorganic filler for the fabrication of electrolyte membranes based on the biopolymer SA. This study involves two main aspects: (i) the synthesis of biomembrane composites including SA, SA/gCN, and SA/S-gCN, and (ii) the analysis of the physical and chemical properties of these SA, SA/gCN, and SA/S-gCN biomembrane composites. The study included the fabrication of SA/S-gCN and SA/gCN membranes using the solution casting process, followed by drying at certain temperatures. The SA/gCN and SA/S-gCN biomembranes were examined using FTIR and XRD analysis to determine their physical structure. The performance of these membranes was evaluated using several tests, such as water absorption, swelling ratio, proton conductivity, and ion exchange capacity.

2. Experimental Section

2.1 Chemicals

Melamine (Sigma Aldrich) and ammonium chloride (NH₄Cl) were used as precursors for gCN synthesis. Other chemicals such as 1,4-butanediol and dimethyl sulfoxide (DMSO) were also obtained from Sigma Aldrich for the sulfonation process of gCN. Sodium chloride, alginate (ACROS ORGANICS), were used as base polymers for SA synthesis, while deionized water served as a solvent for biomembrane preparation. Sodium chloride (NaCl) and sodium hydroxide (NaOH) were purchased from R&M Chemicals for ion exchange capacity analysis. Phenolphthalein was acquired from Bendosen Laboratory Chemicals and used as an indicator.

2.2 Preparation of gCN and S-gCN Fillers

The gCN material was produced by subjecting a mixture of melamine and NH₄Cl to a two-step calcination process, with a mass ratio of 1:4. A total of 5 g of melamine and 20 g of NH₄Cl were introduced into a crucible equipped with a cover. The mixture was then subjected to a heating process in a furnace, where the temperature was gradually increased at a rate of 5 °C per minute until it reached 550 °C. The heating process lasted for 4 hours. Afterward, the crucible was removed from the furnace and let to cool down to the ambient temperature. The collected sample was ground

using a mortar and pestle [17]. Subsequently, the sample was reinserted into the furnace for an extra duration of 2 hours, maintaining the same temperature and heating rate [18]. Next, 1 g of the produced gCN powder was dispersed in 20 mL of DMSO solvent. Then, 0.5 mL of 1,4-butanediol and 0.2 g of NaOH were added to the gCN/DMSO mixture. The mixture was heated to 105 °C and stirred for 6 hours. The resulting S-gCN powder was rinsed several times with hot ethanol, collected by centrifugation, and dried at 80 °C under vacuum. The preparation method for S-gCN is summarized in Figure 1.

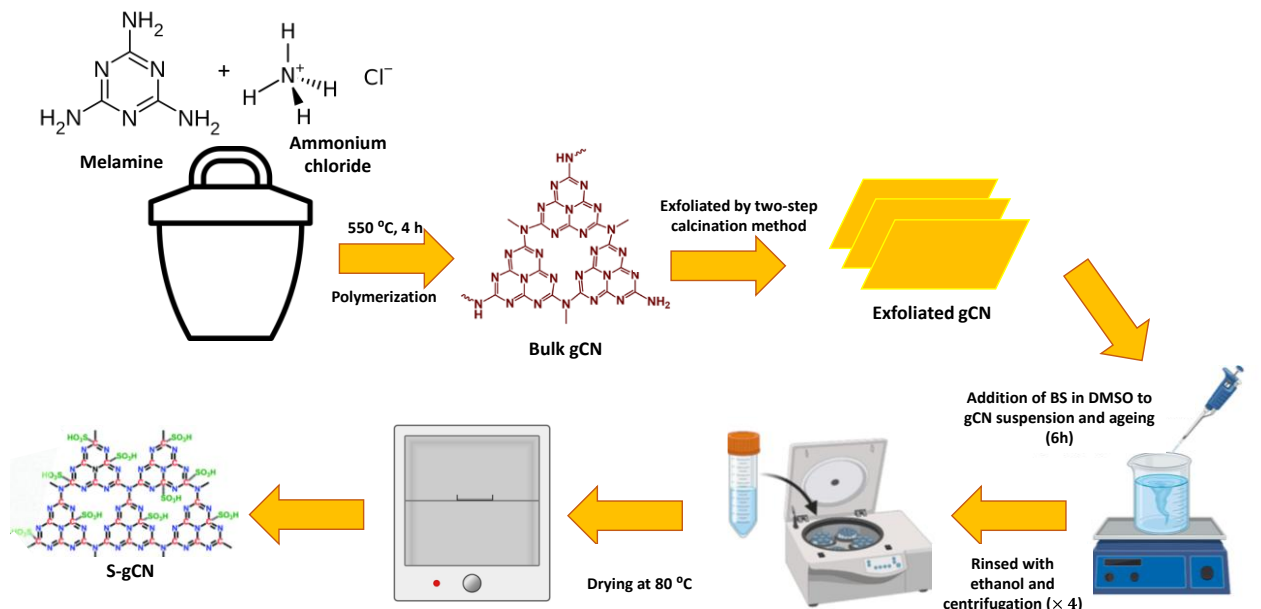


Fig. 1. Preparation method of gCN and S-gCN fillers

2.3 Preparation of SA/S-gCN Biomembrane Composite

The SA/S-gCN composite biomembrane was prepared as described below. SA powder was dissolved in deionized water at room temperature to produce a 3 w/v % polymer solution. Then, 2 wt.% of S-gCN powder was dispersed into the SA polymer solution using the sonication method for 2 hours. After that, the mixture solution was dried at 60 °C for 12 hours. Next, the sample was subjected to annealing at a temperature of 80 °C for 30 minutes to ensure complete dryness of the biomembrane, while maintaining its flexibility and preventing it from becoming swollen. Then, the resulting composite biomembrane SA/S-gCN was externally cross-linked using a glutaraldehyde/glycerol (GA/Gly) solution to reduce the hydrophilic nature of the SA polymer. The SA/S-gCN membrane was immersed in the GA/Gly solution for 30 minutes. The concentration for the GA solution was set for 15%, while the Gly solution concentration was 5%. Finally, the cross-linked SA/S-gCN membrane was air-dried at room temperature. The procedure for preparing SA/S-gCN biomembrane is outlined in Figure 2. This step was repeated using gCN as a filler and without filler to produce SA/gCN membrane and SA membrane, respectively.

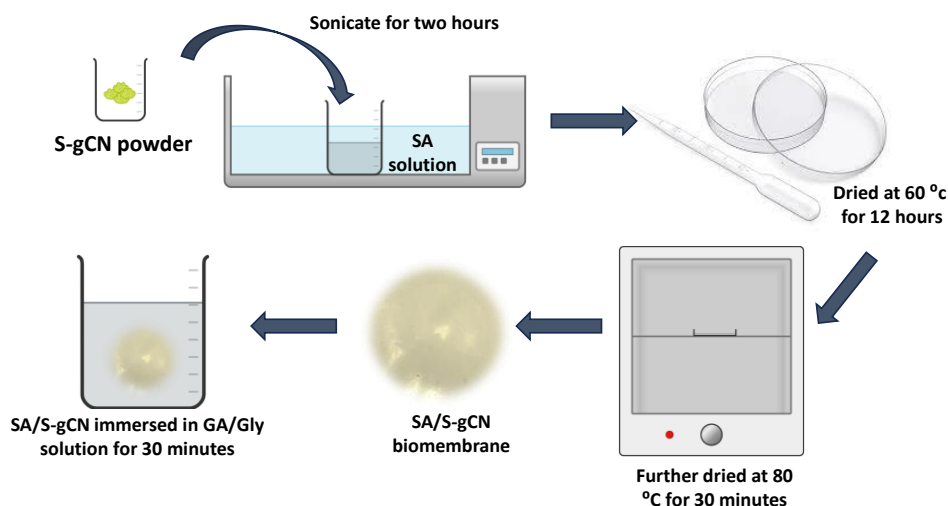


Fig. 2. Preparation method of SA/S-gCN biomembrane

2.4 Physical Characterization

FTIR analysis was conducted to determine the functional groups present in the SA membrane, SA/gCN membrane, and SA/S-gCN membrane. The wavelength range for FTIR was within 4000-500 cm^{-1} . All samples were tested in their as-prepared solid state without additional treatments. The types of chemical bonds and functional groups in each sample varied according to the peaks in their respective spectra. XRD analysis was also performed to determine the crystallinity level of the samples using a Bruker/D8 Advanced model with Cu-K α radiation in the 2θ diffraction range from 5° to 80°. The microstructure and morphology of the samples were observed using field-emission scanning electron microscopy (FESEM) (Carl Zeiss, Gemini).

2.5 Measurement of Water Uptake and Swelling Ratio

The water uptake and swelling ratio of the membrane are important parameters, and they can be measured by observing changes in the weight and thickness of the membrane in wet and dry states. The membrane was immersed in deionized water for 24 hours at room temperature before conducting the water uptake test. The weight and thickness of the membrane in the wet state were recorded. Next, the wet membrane was dried at 100 °C, and the weight and thickness of the dry membrane were also recorded. The water uptake and swelling ratio are calculated using Eq. (1) and Eq. (2) [7].

$$\text{Water uptake} = \frac{W_w - W_d}{W_d} \times 100\% \quad (1)$$

$$\text{Swelling ratio} = \frac{T_w - T_d}{T_d} \times 100\% \quad (2)$$

Where W_w and T_w represent the weight and thickness of the membrane after immersion in deionized water, while W_d and T_d represent the weight and thickness of the membrane after drying. Water uptake and swelling ratio tests were conducted three times to confirm the reproducibility of the membrane in this performance test.

2.6 Measurement of Ion Exchange Capacity

Ion Exchange Capacity (IEC) study is essential, particularly in DMFC technology, as it offers valuable information on the efficiency of a membrane in undergoing ion exchange processes with ions already present. This analysis ultimately determines the maximum amount of cations that can be accumulated inside the membrane. The titration method is often used for IEC analysis. The membrane was immersed in a 2M NaCl solution for 24 hours to facilitate the complete release of H⁺ ions from the membrane into the NaCl solution. After that, the membrane was subjected to a drying process in an oven at a temperature of 100 °C for 24 hours. The resulting weight of the membrane after drying, referred to as W_d , was carefully measured and recorded. The NaCl solution was subjected to titration with a 0.01M NaOH solution, using phenolphthalein as an indicator [19]. The IEC value is calculated using Eq. (3).

$$\text{IEC} = \frac{\text{Volume of NaOH used} \times \text{NaOH Concentration}}{W_d} \quad (3)$$

2.7 Measurement of Proton Conductivity

Proton conductivity for all membranes was determined using a four-probe conductivity cell connected to a potentiostat (WonATech), functioning in a frequency range from 1 MHz to 0.1 Hz. Membranes (with dimensions of 4 cm×1 cm) were immersed in deionized water for at least 24 hours at room temperature to achieve 100% relative humidity. Hydrated membranes assist in the proton activation process. The potentiostat operates to obtain voltage-current plots [20]. The slope of the straight line represents the resistance within the membrane. The resistance values are then incorporated into Eq. (4) to determine the proton conductivity of the membrane.

$$\text{Proton conductivity, } \sigma = \frac{L \text{ (cm)}}{R \text{ } (\Omega) \times A \text{ (cm}^2\text{)}} \quad (4)$$

Where L represents the length of the cut biomembrane, R is the resistance of the membrane, and A is the area of the membrane [21]. Proton conductivity tests were conducted three times to confirm the reproducibility of the membrane in the same test.

3. Results and Discussion

3.1 Physical Observation

Polymer electrolyte membranes based on SA with different fillers (gCN and S-gCN) were observed physically, and images of each membrane are depicted in Figure 3. The pure SA membrane exhibits a transparent and thin film, while gCN and S-gCN fillers have transformed the membranes from transparent to white and physically denser. However, all membranes remain flexible and homogeneous.

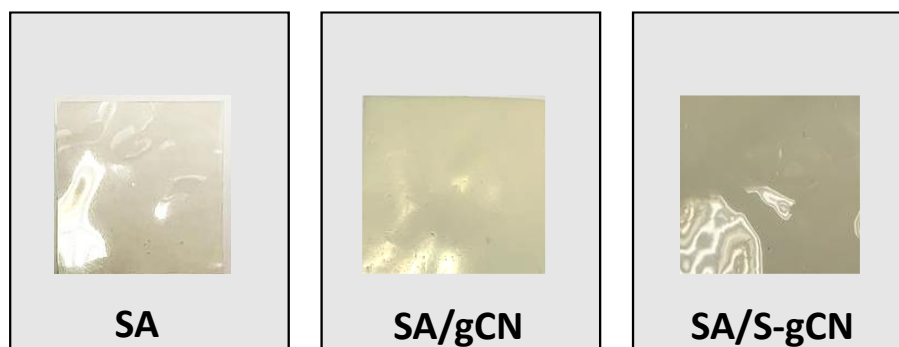


Fig. 3. Physical observation of SA membrane with gCN and S-gCN fillers

3.2 FTIR and XRD Analysis

Figure 4a shows the X-ray diffraction (XRD) patterns for the cross-linked SA membrane, SA/gCN membrane, and SA/S-gCN membrane. As indicated, all samples exhibit an amorphous structure. The presence of cross-linking and plasticizing agents enhances the dominance of the amorphous structure. The XRD pattern for the SA membrane shows distinct diffraction peaks at an angle of $2\theta=13.8^\circ$, indicating the weak crystallinity of the SA membrane, consistent with the previous report [22]. The appearance of clear diffraction peaks at $2\theta=27.7^\circ$ confirms the well-dispersion of gCN filler within the SA polymer matrix. The presence of the peak at $2\theta=27.7^\circ$ also corresponds to the diffraction plane (002) of the overlay 2D layers of gCN [23]. For the SA/S-gCN membrane, the diffraction peaks shifted to $2\theta=28.1^\circ$. This is attributed to the presence of some amorphous regions in the S-gCN sheets [24]. Compared to gCN, the crystallinity of S-gCN is reported to be 50% higher based on the peak intensity. The FTIR analysis was also conducted to identify the functional groups present in the SA, SA-gCN, and SA/S-gCN membranes (Figure 4b). Common peaks for the SA polymer are observed at 3339 cm^{-1} (vibrational stretching of OH groups), 1636 cm^{-1} and 1410 cm^{-1} (vibrational stretching of symmetrical and asymmetrical COO^- groups in carboxylate salts), and 1412 cm^{-1} and 1090 cm^{-1} (vibrational stretching of C-O-C groups) [25]. Peaks around $1028\text{-}948\text{ cm}^{-1}$ are recognized as the peaks of the polysaccharide group (C-C vibration, C-O stretching, and C-H bending). Shaari *et al.*, [22] reported glycerol having major groups such as OH stretching at 3290 cm^{-1} , C-H stretching at 2936 cm^{-1} , and C-O-C stretching at 1417 cm^{-1} , while Hakim *et al.*, [26] reported several major peaks for glutaraldehyde at 3300 cm^{-1} , 2930 cm^{-1} , and 1700 cm^{-1} (C=O group). In the SA spectrum, some major peaks for glutaraldehyde and glycerol overlap with those for pure SA polymer. For the SA/gCN sample, typical spectrum peaks related to the vibration of triazine units, tri-s-triazine units, and -NH₂/-NH- groups are found at 815 cm^{-1} , $1240\text{-}1700\text{ cm}^{-1}$, and 3300 cm^{-1} , respectively [23,27]. In the SA/S-gCN membrane, vibrational peaks appear at 1030 and 3300 cm^{-1} , corresponding to the -SO₃H group vibration and -OH stretching vibration, respectively [23].

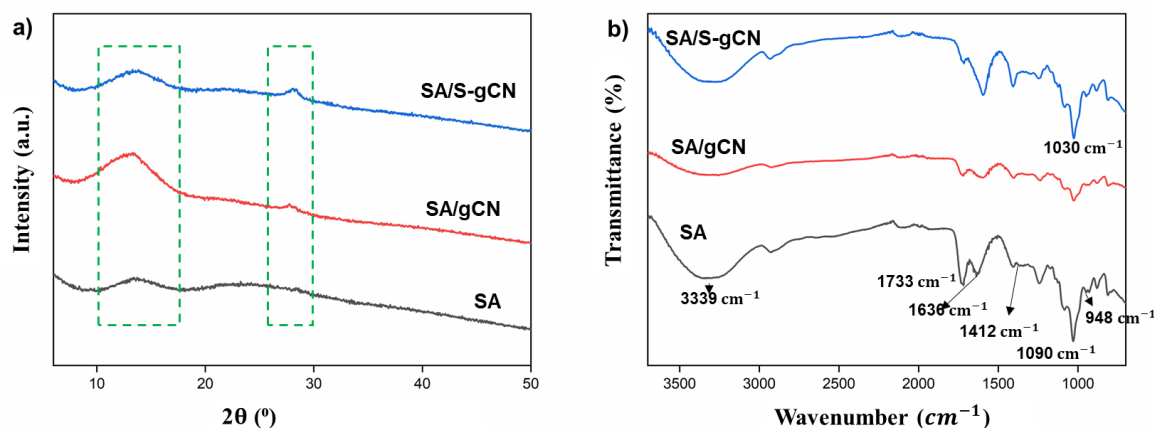


Fig. 4. a) X-ray diffraction patterns of SA, SA/gCN, and SA/S-gCN membranes and b) FTIR spectra of SA, SA/gCN, and SA/S-gCN membranes

3.3 FESEM Analysis

Figure 5 shows the FESEM morphology of SA, SA/gCN, and SA/S-gCN membranes. The FESEM image of the pristine SA membrane reveals a smooth surface with minor wrinkles, indicative of a compact structure. This morphology is likely a result of strong hydrogen bonding within the polysaccharide chains. However, some inhomogeneities in the membrane structure are evident, possibly due to inconsistencies during membrane preparation. Similar findings have been reported in previous studies on sodium alginate membranes, where the compact and smooth morphology typically results in lower water uptake and limited pathways for proton transport [7]. Consequently, this compact structure is associated with reduced proton conductivity. The introduction of g-CN into the SA matrix results in a rougher surface with visible g-CN particles embedded within the membrane (Figure 5b). While this inclusion increases the surface area and introduces potential pathways for proton transport, the uneven distribution of g-CN particles could lead to property variations across different regions of the membrane. Studies in the literature involving g-CN additives in polymer membranes report similar improvements in surface roughness and proton conductivity due to enhanced water retention and proton transfer efficiency. However, the uneven particle dispersion observed in the SA/gCN membrane may create localized regions with inconsistent conductivity, potentially limiting overall membrane performance [28].

The FESEM image of the SA/S-gCN membrane (Figure 5c) exhibits the most pronounced surface roughness and a higher density of embedded particles compared to the other samples. The incorporation of sulfonated g-CN introduces sulfonic acid groups, which are known to facilitate proton conduction. Additionally, the SA/S-gCN membrane shows a relatively more uniform particle distribution than the SA/gCN membrane, although some particle clustering persists. These findings correlated with studies on sulfonated fillers, where the presence of functional groups like sulfonic acids significantly improves proton mobility through the Grotthuss mechanism. The uniform distribution of S-gCN particles enhances membrane performance by providing consistent pathways for proton transport, making the SA/S-gCN composite a promising candidate for improved proton conductivity. The observed increase in surface roughness and surface area in the SA/gCN and SA/S-gCN membranes directly correlates with their potential to enhance proton conductivity. Higher surface roughness facilitates greater water retention, which is essential for creating a medium that supports proton transport. Furthermore, the sulfonic acid groups in the S-gCN particles significantly

enhance proton conduction by acting as proton-accepting sites, enabling efficient proton mobility through the membrane.

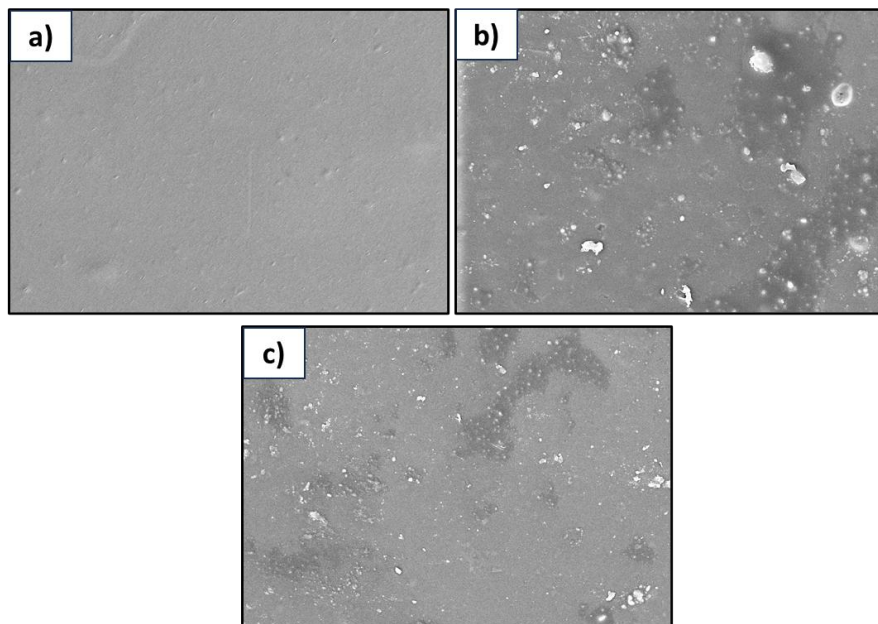


Fig. 5. FESEM images for SA, SA/gCN, and SA/S-gCN membranes

3.4 Water Uptake, Swelling Ratio, and Ion Exchange Capacity

Water absorption is a critical factor in polymer electrolyte membranes (PEMs) as it influences proton transfer via the Grotthuss and Vehicular mechanisms. In this study, the uncross-linked SA membrane dissolved completely in deionized water, indicating its high-water solubility and poor mechanical stability. This result aligns with findings from other studies, where uncross-linked sodium alginate membranes exhibited excessive swelling or dissolution due to their hydrophilic nature. Only the cross-linked SA membranes could be evaluated for water uptake, highlighting the necessity of cross-linking to improve membrane stability. The percentage of water uptake and swelling ratio are illustrated in Figure 6a. The SA/S-gCN membrane demonstrated a lower water uptake and swelling ratio compared to SA/gCN and pure SA membranes. This reduction is primarily attributed to the S-gCN filler, which enhances hydrogen bonding with the SA polymer matrix and constrains the ionic pathways. These findings are consistent with previous studies where fillers such as sulfonated carbon nanotubes or other sulfonated materials reduced water uptake and swelling by improving interfacial adhesion and restricting water mobility [29]. The controlled water uptake in the SA/S-gCN membrane ensures adequate hydration for proton conduction while maintaining structural integrity, a key requirement for PEMs in DMFC application.

In terms of ion exchange capacity (IEC), the SA/S-gCN membrane exhibited the highest value, surpassing those of the SA/gCN and pure SA membranes. The higher IEC is a result of the acid-base interactions between the amino groups of S-gCN and the SA polymer, along with the presence of sulfonic acid (SO_3H) groups in the S-gCN filler. Similar trends have been reported in studies utilizing sulfonated fillers, where the addition of SO_3H groups significantly enhanced IEC values by increasing the availability of proton-conducting sites [30]. The IEC values for SA/S-gCN, SA/gCN, and pure SA were 41.69%, 33.22%, and 25.08% (as shown in the pie chart in Figure 6b), respectively, demonstrating the effectiveness of S-gCN in improving the membrane's proton exchange capacity.

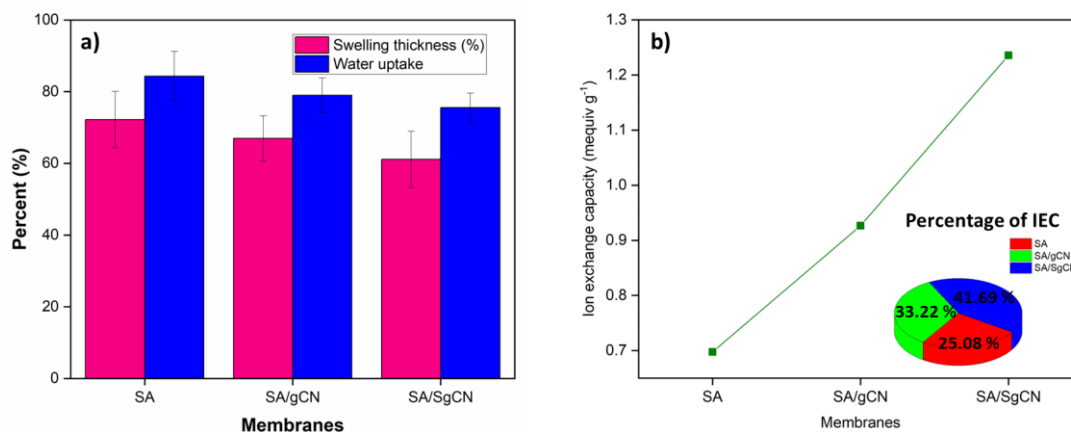


Fig. 6. Percentage of water uptake and swelling ratio of all prepared membranes, and b) Ion exchange capacity of SA, SA/gCN and SA/S-gCN membranes

3.5 Proton Conductivity

Proton conductivity is a critical parameter in evaluating the performance of polymer electrolyte membranes (PEMs), as it directly impacts the efficiency of fuel cells. The ability of a membrane to facilitate proton transfer is influenced by its chemical composition, structure, and the nature of interactions between its components. Table 1 highlights the proton conductivity values for the SA, SA/gCN, and SA/S-gCN membranes, with the SA/S-gCN membrane exhibiting the highest conductivity of 8.67 mS cm^{-1} , followed by SA/gCN (8.37 mS cm^{-1}) and pure SA (7.78 mS cm^{-1}). The incorporation of fillers such as gCN and S-gCN significantly impacts the proton conductivity of the membranes. The SA/gCN membrane demonstrates an improvement in conductivity over the pure SA membrane due to the increased surface area provided by the gCN filler, which promotes better water retention and creates additional pathways for proton transport. However, its conductivity is lower than that of the SA/S-gCN membrane due to the absence of proton-hopping functional groups like SO_3H [30].

In the SA/S-gCN membrane, the sulfonated gCN filler introduces SO_3H groups, which serve as proton-hopping sites. These groups facilitate acid-base interactions with the carboxylate groups in the SA polymer, strengthening the membrane structure and forming continuous proton transfer channels. This acid-base interaction not only improves the membrane's proton conductivity but also enhances its stability by reducing water uptake and swelling. Such interactions have been widely reported in the literature, where sulfonated fillers enhance proton conductivity in biopolymer matrices by increasing the number of active sites and improving proton mobility. Proton transport in PEMs generally occurs through two primary mechanisms which are the Grotthuss mechanism and Vehicular mechanism. In this Grotthuss mechanism, protons "hop" between hydrogen-bonded water molecules. SO_3H groups play a significant role by providing active sites for proton hopping. The presence of SO_3H groups in the SA/S-gCN membrane facilitates this mechanism, as they create a network of hydrogen bonds that act as proton transfer channels. The higher density of these functional groups in the SA/S-gCN membrane enhances its proton conductivity compared to the SA and SA/gCN membranes. While for Vehicle mechanism, the protons were move via hydrated ions such as H_3O^+ . The water uptake of the membrane determines the availability of hydration layers necessary for vehicular transport. While excessive water uptake can lead to membrane swelling and loss of mechanical stability, controlled water retention in the SA/S-gCN membrane ensures an optimal hydration environment for proton transport [31].

The observed proton conductivity values align with trends reported in previous studies. Membranes incorporating sulfonated fillers or functionalized inorganic additives consistently show higher conductivity due to the synergistic effect of increased functional group density and improved water management. For instance, sulfonated graphene oxide [32,33] and carbon nanotubes have been shown to improve both conductivity and structural stability in PEMs, mirroring the enhancements observed in the SA/S-gCN membrane. The superior proton conductivity of the SA/S-gCN membrane underscores its potential for DMFC applications. However, achieving even higher conductivity may require further optimization, such as ensuring uniform filler dispersion and exploring additional functionalization of the biopolymer matrix. Future studies could also investigate the long-term stability of these membranes under operational conditions, as well as their performance under varying humidity and temperature levels.

Table 1
Proton conductivity values for SA, SA/gCN, and SA/S-gCN biomembranes

Membranes	Value of proton conductivity (mS cm ⁻¹)
SA	7.78
SA/gCN	8.37
SA/S-gCN	8.67

4. Conclusion and Future Directions

Biomembrane composites consisting of SA with S-gCN as a potential inorganic filler have been successfully explored as an alternative membrane for DMFC applications. Physical characterization through FTIR and XRD analyses has confirmed the successful incorporation of S-gCN into the SA biopolymer matrix. FTIR analysis has validated the interaction between the SA biopolymer and S-gCN due to the presence of the main spectra of both SA and S-gCN in the biocomposite. Hydrogen bonding interactions between SA and S-gCN can enhance the interfacial bonding between SA and S-gCN, thereby improving the proton conductivity of the biocomposite. This study found that S-gCN as an inorganic filler in the SA biopolymer can reduce water uptake percentage, enhance ion exchange capacity, and improve proton conductivity. To achieve higher conductivity may require further optimization, such as ensuring uniform filler dispersion and exploring additional functionalization of the biopolymer matrix. Future studies could also investigate the long-term stability of these membranes under operational conditions, as well as their performance under varying humidity and temperature levels. The SA/S-gCN membrane exhibits superior performance with lower water uptake and higher ion exchange capacity than other membranes. This combination of properties is crucial for achieving high power output and durability in DMFCs. Furthermore, using bio-based SA and S-gCN fillers aligns with the growing demand for sustainable and environmentally friendly energy solutions. While this study demonstrates the potential of SA/S-gCN membranes, further investigations are necessary to fully assess their long-term stability, mechanical properties, and overall performance in practical DMFC applications. Future work could focus on optimizing the fabrication process to ensure uniform filler distribution and to minimize any potential clustering of S-gCN particles, which could impact proton conductivity. Additionally, exploring other bio-based or functionalized additives could further enhance membrane properties.

Acknowledgment

This research was fully supported by Universiti Kebangsaan Malaysia (UKM) and the Ministry of Higher Education through financial assistance from the Fundamental Research Grant Scheme FRGS/1/2021/STG05/UKM/02/10

References

- [1] Nasser, Ruhilin, Siti Khadijah Hubadillah, Mohd Hafiz Dzarfan Othman, and Arif Akmal Mohamed Hassan. "Fabrication and Characterization of Low-Cost Poly (Vinyl Alcohol) Composite Membrane for Low Temperature Fuel Cell Application." *Journal of Applied Membrane Science & Technology* 22, no. 1 (2018). <https://doi.org/10.11113/amst.v22n1.128>
- [2] Pan, Zhefei, Yanding Bi, and Liang An. "Performance characteristics of a passive direct ethylene glycol fuel cell with hydrogen peroxide as oxidant." *Applied energy* 250 (2019): 846-854. <https://doi.org/10.1016/j.apenergy.2019.05.072>
- [3] Rajeswara, Sarveshini, Muliani Mansor, Nurfatehah Wahyuny Che Jusoh, Azran Mohd Zainoodin, Khairunnisa Mohd Pa'ad, and Shinya Yamanaka. "The Effects of Calcination Temperature of Nickel Supported on Candle Soot towards Ethanol Oxidation Reaction (EOR)." *Journal of Research in Nanoscience and Nanotechnology* 8, no. 1 (2023): 23-30. <https://doi.org/10.37934/jrnn.8.1.2330>
- [4] You, P. Y., S. K. Kamarudin, and M. S. Masdar. "Improved performance of sulfonated polyimide composite membranes with rice husk ash as a bio-filler for application in direct methanol fuel cells." *International Journal of Hydrogen Energy* 44, no. 3 (2019): 1857-1866. <https://doi.org/10.1016/j.ijhydene.2018.11.166>
- [5] Junoh, Hazlina, Juhana Jaafar, Nik Abdul Hadi M. Nordin, Ahmad F. Ismail, Mohd HD Othman, Mukhlis A. Rahman, Farhana Aziz, Norhaniza Yusof, and Syarifah Noor S. Sayed Daud. "Porous polyether sulfone for direct methanol fuel cell applications: Structural analysis." *International Journal of Energy Research* 45, no. 2 (2021): 2277-2291. <https://doi.org/10.1002/er.5921>
- [6] Daud, Syarifah Noor Syakiylla Sayed, Muhamad Noorul Anam Mohd Norddin, Juhana Jaafar, and Rubita Sudirman. "Fabrication, Properties, and Performance of Polymer Nanocomposite Ion Exchange Membranes for Fuel Cell Applications: A Review." *Journal of Applied Membrane Science & Technology* 26, no. 1 (2022): 11-49. <https://doi.org/10.11113/amst.v26n1.230>
- [7] Shaari, N., and S. K. Kamarudin. "Sodium alginate/alumina composite biomembrane preparation and performance in DMFC application." *Polymer Testing* 81 (2020): 106183. <https://doi.org/10.1016/j.polymertesting.2019.106183>
- [8] Raduwan, Nor Fatina, Norazuwana Shaari, Siti Kartom Kamarudin, Mohd Shahbudin Masdar, Rozan Mohamad Yunus, and Ajaz Ahmad Wani. "Advances, progress and challenges of NiCo2O4-based composite materials for direct methanol fuel cell applications: A critical review." *International Journal of Green Energy* 21, no. 14 (2024): 3391-3413. <https://doi.org/10.1016/B978-0-443-15740-0.00095-1>
- [9] Shaari, N., and S. K. Kamarudin. "Chitosan and alginate types of bio-membrane in fuel cell application: An overview." *Journal of Power Sources* 289 (2015): 71-80. <https://doi.org/10.1016/j.jpowsour.2015.04.027>
- [10] Yusoff, Y. N., N. Shaari, M. A. Mohamed, K. S. Loh, and S. K. Kamarudin. "Enhanced proton conductivity and mechanical stability of crosslinked sodium alginate as a biopolymer electrolyte membrane in fuel cell application." In *IOP Conference Series: Earth and Environmental Science*, vol. 1372, no. 1, p. 012104. IOP Publishing, 2024. <https://doi.org/10.1088/1755-1315/1372/1/012104>
- [11] Shaari, N., S. K. Kamarudin, S. Basri, L. K. Shyuan, M. S. Masdar, and D. Nordin. "Enhanced mechanical flexibility and performance of sodium alginate polymer electrolyte bio-membrane for application in direct methanol fuel cell." *Journal of Applied Polymer Science* 135, no. 37 (2018): 46666. <https://doi.org/10.1002/app.46666>
- [12] Ping-Ping, Zuo, Zhang Yu-Long, Feng Hua-Feng, Xia Wei, Zhang Wen-Qing, and Wang Ming-Zhang. "Fabrication and properties of graphene oxide-reinforced Carrageenan Film." *Chemical Journal of Chinese Universities-Chinese* 34, no. 3 (2013): 692-697. <https://doi.org/10.1109/GLOCOM.2014.7036888>
- [13] Zhang, Wei, Zhejun Yu, Qiufang Qian, Zhennan Zhang, and Xinping Wang. "Improving the pervaporation performance of the glutaraldehyde crosslinked chitosan membrane by simultaneously changing its surface and bulk structure." *Journal of Membrane Science* 348, no. 1-2 (2010): 213-223. <https://doi.org/10.1016/j.memsci.2009.11.003>
- [14] Shaari, Norazuwana, and Siti Kartom Kamarudin. "Recent advances in additive-enhanced polymer electrolyte membrane properties in fuel cell applications: An overview." *International Journal of Energy Research* 43, no. 7 (2019): 2756-2794. <https://doi.org/10.1002/er.4348>
- [15] Ajiboye, Timothy O., Alex T. Kuvarega, and Damian C. Onwudiwe. "Graphitic carbon nitride-based catalysts and their applications: A review." *Nano-Structures & Nano-Objects* 24 (2020): 100577. <https://doi.org/10.1016/j.nanoso.2020.100577>
- [16] Gang, Mingyue, Guangwei He, Zhen Li, Keteng Cao, Zongyu Li, Yongheng Yin, Hong Wu, and Zhongyi Jiang. "Graphitic carbon nitride nanosheets/sulfonated poly (ether ether ketone) nanocomposite membrane for direct methanol fuel cell application." *Journal of Membrane Science* 507 (2016): 1-11. <https://doi.org/10.1016/j.memsci.2016.02.004>
- [17] Dang, Yinping, Qi Hu, Ping He, and Tongyan Ren. "Tailoring the ratio of ammonium chloride and graphitic carbon nitride for high photocatalytic activity." *Journal of Molecular Structure* 1209 (2020): 127961. <https://doi.org/10.1016/j.molstruc.2020.127961>
- [18] Kumar, Arun, Sonal Singh, and Manika Khanuja. "Temperature based morphological study of graphitic carbon nitride for photocatalytic application." In *AIP Conference Proceedings*, vol. 2276, no. 1. AIP Publishing, 2020. <https://doi.org/10.1063/5.0025725>

- [19] Vijitha, Raagala, Kasula Nagaraja, Marlia M. Hanafiah, Kummara Madhusudana Rao, Katta Venkateswarlu, Sivarama Krishna Lakkaboyana, and Kummari SV Krishna Rao. "Fabrication of eco-friendly polyelectrolyte membranes based on sulfonate grafted sodium alginate for drug delivery, toxic metal ion removal and fuel cell applications." *Polymers* 13, no. 19 (2021): 3293. <https://doi.org/10.3390/polym13193293>
- [20] Shaari, Norazuwana, Siti Kartom Kamarudin, and Zulfirdaus Zakaria. "Potential of sodium alginate/titanium oxide biomembrane nanocomposite in dmfc application." *International Journal of Energy Research* 43, no. 14 (2019): 8057-8069. <https://doi.org/10.1002/er.4801>
- [21] Cozzi, Dafne, Catia de Bonis, Alessandra D'Epifanio, Barbara Mecheri, Ana C. Tavares, and Silvia Licocchia. "Organically functionalized titanium oxide/Nafion composite proton exchange membranes for fuel cells applications." *Journal of Power Sources* 248 (2014): 1127-1132. <https://doi.org/10.1016/j.jpowsour.2013.10.070>
- [22] Shaari, N., S. K. Kamarudin, S. Basri, L. K. Shyuan, M. S. Masdar, and D. Nordin. "Enhanced mechanical flexibility and performance of sodium alginate polymer electrolyte bio-membrane for application in direct methanol fuel cell." *Journal of Applied Polymer Science* 135, no. 37 (2018): 46666. <https://doi.org/10.1002/app.46666>
- [23] Lu, Yao, Yue Liu, Na Li, Zhaoxia Hu, and Shouwen Chen. "Sulfonated graphitic carbon nitride nanosheets as proton conductor for constructing long-range ionic channels proton exchange membrane." *Journal of Membrane Science* 601 (2020): 117908. <https://doi.org/10.1016/j.memsci.2020.117908>
- [24] He, Xueyi, Guangwei He, Anqi Zhao, Fei Wang, Xunli Mao, Yongheng Yin, Li Cao, Bei Zhang, Hong Wu, and Zhongyi Jiang. "Facilitating proton transport in nafion-based membranes at low humidity by incorporating multifunctional graphene oxide nanosheets." *ACS Applied Materials & Interfaces* 9, no. 33 (2017): 27676-27687. <https://doi.org/10.1021/acsami.7b06424>
- [25] Shaari, Norazuwana, and Siti Kartom Kamarudin. "Characterization studies of sodium alginate/sulfonated graphene oxide based polymer electrolyte membrane for direct methanol fuel cell." *Malaysian Journal of Analytical Sciences* 21, no. 1 (2017): 113-118. <https://doi.org/10.17576/mjas-2017-2101-13>
- [26] Hakim S, Abdul, Satria Mihardi, and Abdul Rais. "Characterization of Glutaraldehyde Composition on PVA Enzyme Coated PVC-KTPCLPB Membrane with XRD, UV-VIS, SEM-EDS, and FTIR." *Rasayan J. Chem* 15, no. 4 (2022): 2714-2723. <https://doi.org/10.31788/RJC.2022.1547073>
- [27] Yan, Jing, Chenjuan Zhou, Peiran Li, Binhe Chen, Shishen Zhang, Xiaoping Dong, Fengna Xi, and Jiyang Liu. "Nitrogen-rich graphitic carbon nitride: controllable nanosheet-like morphology, enhanced visible light absorption and superior photocatalytic performance." *Colloids and Surfaces A: Physicochemical and Engineering Aspects* 508 (2016): 257-264. <https://doi.org/10.1016/j.colsurfa.2016.08.067>
- [28] Yogarathinam, Lukka Thuyavan, Juhana Jaafar, Ahmad Fauzi Ismail, Hazlina Junoh, Alireza Samavati, Pei Sean Goh, Arthanareeswaran Gangasalam, and Jerome Peter. "Synthesis and characterization of conductive polymer coated graphitic carbon nitride embedded sulfonated poly (ether ether ketone) membranes for direct methanol fuel cell applications." *International Journal of Energy Research* 45, no. 11 (2021): 16649-16666. <https://doi.org/10.1002/er.6911>
- [29] Shirdast, Abbas, Alireza Sharif, and Mahdi Abdollahi. "Effect of the incorporation of sulfonated chitosan/sulfonated graphene oxide on the proton conductivity of chitosan membranes." *Journal of Power Sources* 306 (2016): 541-551. <https://doi.org/10.1016/j.jpowsour.2015.12.076>
- [30] Velayutham, Parthiban, and A. K. Sahu. "Graphitic carbon nitride nanosheets—nafion as a methanol barrier hybrid membrane for direct methanol fuel cells." *The Journal of Physical Chemistry C* 122, no. 38 (2018): 21735-21744. <https://doi.org/10.1021/acs.jpcc.8b06042>
- [31] Niu, Ruiting, Lingqian Kong, Lanyue Zheng, Haixia Wang, and Haifeng Shi. "Novel graphitic carbon nitride nanosheets/sulfonated poly (ether ether ketone) acid-base hybrid membrane for vanadium redox flow battery." *Journal of Membrane Science* 525 (2017): 220-228. <https://doi.org/10.1016/j.memsci.2016.10.049>
- [32] Yusoff, Yusra Nadzirah, Kee Shyuan Loh, Wai Yin Wong, Wan Ramli Wan Daud, and Tian Khoon Lee. "Sulfonated graphene oxide as an inorganic filler in promoting the properties of a polybenzimidazole membrane as a high temperature proton exchange membrane." *International Journal of Hydrogen Energy* 45, no. 51 (2020): 27510-27526. <https://doi.org/10.1016/j.ijhydene.2020.07.026>
- [33] Yusoff, Yusra Nadzirah, Kee Shyuan Loh, and Wai Yin Wong. "Kesan Pengisi Titanium Dioksida Dalam Membran Komposit Polibenzimidazol-Grafina Oksida Bersulfonat Bagi Aplikasi Pemfc Bersuhu Tinggi: The Effect Of Titanium Dioxide Filler In Polybenzimidazole-Sulfonated Graphene Oxide Composite Membrane For High-Temperature Pemfc Applications." *Jurnal Teknologi* 86, no. 1 (2024): 53-62. <https://doi.org/10.11113/jurnalteknologi.v86.20075>